Resonant Andreev reflection in a normal-metal/quantum-dot/superconductor system with coupled Majorana bound states*

Su-Xin Wang(王素新)[1,2], Yu-Xian Li(李玉现)[1], and Jian-Jun Liu(刘建军)[1,3,†]

[1] College of Physical Science and Information Engineering and Hebei Advanced Thin Film Laboratory, Hebei Normal University, Shijiazhuang 050024, China

[2] Department of Physics, Hebei Normal University for Nationalities, Chengde 067000, China

[3] Physics Department, Shijiazhuang University, Shijiazhuang 050035, China

(Received 9 October 2015; revised manuscript received 3 December 2015; published online 18 January 2016)

Andreev reflection (AR) in a normal-metal/quantum-dot/superconductor (N–QD–S) system with coupled Majorana bound states (MBSs) is investigated theoretically. We find that in the N–QD–S system, the AR can be enhanced when coupling to the MBSs is incorporated. Fano line-shapes can be observed in the AR conductance spectrum when there is an appropriate QD–MBS coupling or MBS–MBS coupling. The AR conductance is always $e^2/2h$ at the zero Fermi energy point when only QD–MBSs coupling is considered. In addition, the resonant AR occurs when the MBS–MBS coupling roughly equals to the QD energy level. We also find that an AR antiresonance appears when the QD energy level approximately equals to the sum of the QD–MBS coupling and the MBS–MBS coupling. These features may serve as characteristic signatures for the probe of MBSs.

Keywords: Majorana bound states, Andreev reflection, Fano effect, quantum dot

PACS: 73.21.La, 74.45.+c, 73.23.Hk **DOI:** 10.1088/1674-1056/25/3/037304

1. Introduction

A Majorana particle is a fermion that is its own antiparticle and obeys novel non-Abelian statistics, which was proposed by Majorana in 1937.[1,2] Due to their potential applications in topological quantum computation and because of their fundamental interest, Majorana fermions are currently attracting increased attention.[3–9] Recently, it has been reported that Majorana bound states (MBSs) can be realized at the ends of a one-dimensional p-wave superconductor; the proposed system is a semiconductor nanowire with Rashba spin–orbit interaction, to which both a magnetic field and proximity-induced s-wave paired are added.[10,11] Soon after this proposal, several groups have fabricated the semiconductor superconducting wire and observed zero-bias conductance peaks (ZBCP).[3,8,12]

Up to now, the ZBCP is the unique signature that has been observed experimentally to check the existence of MBS. However, the ZBCP could also originate from non-topological physics mechanisms. Fortunately, numerous theoretical and experimental studies exactly illustrate that the quantum dot (QD) structure is a good candidate for the detection of MBSs.[13–24] It has been reported that when a QD is noninteracting and in the resonant tunneling regime, the MBS influences the conductance through the QD by inducing a sharp decrease of the conductance by a factor of 1/2.[14] The nonlocal nature of Majorana fermions can cause novel transport phenomena such as crossed Andreev reflection (CAR), which was earlier proposed in Ref. [25] as a method to probe the nonlocality of a pair of MBSs. A possible probe for Majorana fermions was also suggested in Ref. [26], where two MBSs that are coupled to QDs, which themselves interact with two normal-metal leads, can be tested uniquely using CAR.

On the other hand, in several previous studies, QDs coupled with normal metallic conductors (N) and with superconducting electrode (S) structures have been investigated and it was found that they exhibit interesting transport properties.[27–29] One of these properties is the so-called Andreev reflection (AR).[30,31] In an AR process, an electron with an energy below the supperconducting gap is reflected at the interface as a hole, while a Cooper pair of charge $2e$ is created in the superconducting side of the interface. In the subgap regime ($eV < \Delta$), the tunneling conductance almost entirely originates from the anomalous Andreev channel; such spectroscopy can thus directly probe any in-gap states. For instance, the tunneling conductance has recently been measured in a system comprising indium antimonide nanowires connected to a normal electrode and a superconducting electrode, indicating Majorana-type in-gap states.[8]

Motivated by the existing transport results, in the present work, we consider a spinless QD coupled to an MBS at one

*Project supported by the National Natural Science Foundation of China (Grant Nos. 61176089 and 10974043), the Natural Science Foundation of Hebei Province, China (Grant Nos. A2011205092 and 2014205005), and the Fund for Hebei Normal University for Nationalities, China (Grant No. 201109).

†Corresponding author. E-mail: liujj@mail.hebtu.edu.cn

© 2016 Chinese Physical Society and IOP Publishing Ltd

end of a p-wave superconducting nanowire, and investigate the AR conductance through the QD by adding a normal lead and a superconducting lead. We find that in addition to the resonant behavior of the Andreev tunneling described in the previous investigations,[28] when coupling between the QD and MBSs is incorporated, the AR conductance spectrum has several new features. One example is the Fano effect,[32] which arises from the interference between a discrete state and the continuum, giving rise to the characteristically asymmetric line shapes. In addition, the AR conductance is always $e^2/2h$ at the zero energy point when only QD–MBSs coupling is considered, showing the robust properties of the Majorana fermions. We also discuss under what conditions the resonant AR might appear. Therefore, the AR conductance in such a structure can serve as a characteristic signature in probing MBSs.

The rest of this paper is organized as follows. In Section 2, we introduce the model Hamiltonian of the N–QD–S system with coupled MBSs. In Section 3, we present numerical results for the transport properties and discuss the underlying physical processes. A summary is given in Section 4.

2. Model and method

The N–QD–S system with coupled MBSs is illustrated in Fig. 1. A QD is connected with N and S leads. The QD can be fabricated by applying gate voltages on a two-dimensional electron gas.[33] In addition, a semiconductor nanowire with strong Rashba interaction is subjected to a strong magnetic field $\boldsymbol{B}$ and adhere a proximity-induced s-wave superconductivity, then a pair of MBSs can form at the ends of the nanowire.[2,7] In Fig. 1, the two MBSs are defined as η_1 and η_2. Here, we suppose that the QD is only connected to η_1 and the coupling strength is λ. We assume that the system under consideration is described by the following Hamiltonian:

$$H = H_0 + H_{\rm L} + H_{\rm R} + H_{\rm T}. \tag{1}$$

The QD–Majorana part is described by

$$H_0 = \sum_i \varepsilon_i d_i^\dagger d_i + {\rm i}\varepsilon_{\rm M}\eta_1\eta_2 + (\lambda d - \lambda^* d^\dagger)\eta_1, \tag{2}$$

where ε_i is a tunable gate energy level in the QD which is assumed to have multiple discrete energy levels characterized by the index i, and d_i ($d_i^\dagger$) is the electron annihilation (creation) operator. The second term in Eq. (2), the low-energy effective Hamiltonian for the MBSs, describes the pair of MBSs, η_1 and η_2, generated at the ends of the nanowire and coupled to each other with energy $\varepsilon_{\rm M}$.[25] The last term in Eq. (2) describes the tunneling coupling between the QD and η_1. In Eq. (1), $H_{\rm L}$ describes noninteracting electrons with momentum k and spin σ in the left normal-metal lead; $H_{\rm R}$ describes electrons with momentum p in the right superconducting lead, which has an energy gap Δ; and $H_{\rm T}$ gives the tunneling part of the Hamiltonian. They can be written as

$$H_{\rm L} = \sum_{k,\sigma}(\varepsilon^0_{{\rm L},k} - eV_{\rm L})c^\dagger_{{\rm L},k\sigma}c_{{\rm L},k\sigma}, \tag{3}$$

$$H_{\rm R} = \sum_{p,\sigma}\varepsilon^0_{{\rm R},p}c^\dagger_{{\rm R},p\sigma}c_{{\rm R},p\sigma} + \sum_p\left[\Delta^* c_{{\rm R},p\downarrow}c_{{\rm R},-p\uparrow} + \Delta c^\dagger_{{\rm R},-p\uparrow}c^\dagger_{{\rm R},p\downarrow}\right], \tag{4}$$

$$H_{\rm T} = \sum_{k,\sigma,i}\left[t_{\rm L}c^\dagger_{{\rm L},k\sigma}d_{i\sigma} + t^*_{\rm L}d^\dagger_{i\sigma}c_{{\rm L},k\sigma}\right] + \sum_{p,\sigma,i}\left[t_{\rm R}\,{\rm e}^{{\rm i}eV_{\rm R}\tau}d_{i\sigma}c^\dagger_{{\rm R},p,\sigma} + t^*_{\rm R}\,{\rm e}^{-{\rm i}eV_{\rm R}\tau}d^\dagger_{i\sigma}c_{{\rm R},p,\sigma}\right]. \tag{5}$$

Here, $c^\dagger$ (c) is the creation (annihilation) operator of the electron in the leads, $V_{\rm L}$ is the voltage on the left lead, and $V_{\rm R}$ is the voltage on the right lead. In Eq. (5), t_v ($v = {\rm L},{\rm R}$) is the hopping matrix, which, for simplicity, is assumed to be independent of the states in the leads and the QD.

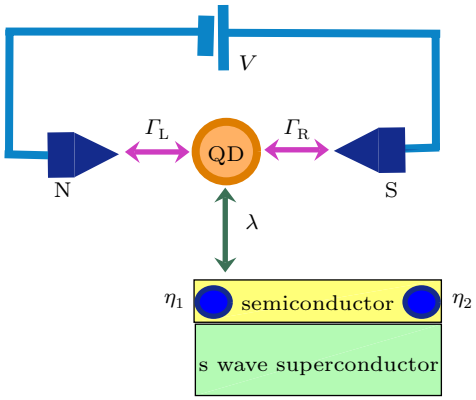


Fig. 1. (color online) Sketch of an N–QD–S system with coupled MBSs. A QD is connected with N and S leads. The QD is also connected to one end of a quantum wire on an s-wave supercunductor surface, which supports an MBS (blue dot) at each end. The two MBSs are defined as η_1 and η_2.

It is helpful to replace the Majorana fermion operators by ordinary fermion operators f and $f^\dagger$, where f creates a fermion and $f^\dagger f =$ odd, even counts the parity of the MBS. In the new representation, we have $\eta_1 = (f^\dagger + f)/\sqrt{2}$ and $\eta_2 = {\rm i}(f^\dagger - f)/\sqrt{2}$ with $\{f, f^\dagger\} = 1$. Accordingly, we can write H_0 in the form

$$H_0 = \sum_i \varepsilon_i d_i^\dagger d_i + \varepsilon_{\rm M}\left(f^\dagger f - \frac{1}{2}\right) + \frac{1}{\sqrt{2}}(\lambda d - \lambda^* d^\dagger)(f^\dagger + f). \tag{6}$$

The electric current can be evaluated from the time evolution of the total electron number in the left lead, $N_{\rm L} = \sum_{k\sigma} c^\dagger_{{\rm L},k\sigma}c_{{\rm L},k\sigma}$, using the expression

$$I = -e\langle\dot{N}_{\rm L}(\tau)\rangle = -({\rm i}e/\hbar)\langle[H, N_{\rm L}]\rangle. \tag{7}$$

Within the nonequilibrium Keldysh–Green function formalism,[28,34] one finds that the current $I = I_{\rm A} + I_{\rm Q}$ is the

sum of two terms: the Andreev current $I_{\rm A}$ and the quasiparticle contribution $I_{\rm Q}$

$$I_{\rm A} = \frac{2e}{h}\int {\rm d}\omega T_{\rm A}(\omega)\left[f_{\rm L}(\omega - eV) - f_{\rm L}(\omega + eV)\right], \quad (8)$$

$$I_{\rm Q} = \frac{2e}{h}\int {\rm d}\omega T_{\rm Q}(\omega)\left[f_{\rm L}(\omega - eV) - f_{\rm R}(\omega)\right]. \quad (9)$$

Here, the Fermi–Dirac distribution function is given by

$$f_{\alpha={\rm L,R}}(\omega \pm eV) = \left\{1 + \exp\left[(\omega \pm eV - E_{\rm F})/k_{\rm B}T\right]\right\}^{-1}, \quad (10)$$

where T is the electrode temperature. The voltage bias V is the difference between the voltages on the left and the right leads: $V = V_{\rm L} - V_{\rm R}$. $E_{\rm F}$ is the Fermi energy. The Fermi function $f_{\rm R}$ for the superconducting lead is that of the zero-gap state, with the gap properties included in the superconductor density of states. Both transmissions $T_{\rm A}$ and $T_{\rm Q}$ are expressed in terms of the QD retarded Green's function $\boldsymbol{G}^{\rm r}_{ij}(\omega)$ in Nambu space.

The Fourier transformed retarded Green's function of the system can be solved using Dyson's equation, $\boldsymbol{G}^{\rm r} = \boldsymbol{G}^{\rm r}_0 + \boldsymbol{G}^{\rm r}_0\boldsymbol{\Sigma}^{\rm r}\boldsymbol{G}^{\rm r}$, where $\boldsymbol{\Sigma}^{\rm r}$ is the self-energy matrix due to the tunneling coupling between the QD and the leads. In the 4×4 generalized Nambu-spin space, the free Green's function $\boldsymbol{G}^{\rm r}_0$ for the QD with the MBSs is given by

$$[\boldsymbol{G}^{\rm r}_0(\omega)]^{-1} = \begin{pmatrix} \omega - \varepsilon_i & 0 & \frac{\lambda^*}{\sqrt{2}} & \frac{\lambda^*}{\sqrt{2}} \\ 0 & \omega + \varepsilon_i & -\frac{\lambda}{\sqrt{2}} & -\frac{\lambda}{\sqrt{2}} \\ \frac{\lambda}{\sqrt{2}} & -\frac{\lambda^*}{\sqrt{2}} & \omega - \varepsilon_{\rm M} & 0 \\ \frac{\lambda}{\sqrt{2}} & -\frac{\lambda^*}{\sqrt{2}} & 0 & \omega + \varepsilon_{\rm M} \end{pmatrix}. \quad (11)$$

The self-energy matrix $\boldsymbol{\Sigma}^{\rm r}$ consists of two parts: $\boldsymbol{\Sigma}^{\rm r} = \boldsymbol{\Sigma}^{\rm r}_{\rm L} + \boldsymbol{\Sigma}^{\rm r}_{\rm R}$. The term $\boldsymbol{\Sigma}^{\rm r}_{\rm L}$ is the self-energy from the coupling between the QD and the left normal-metal lead. The matrix form of $\boldsymbol{\Sigma}^{\rm r}_{\rm L}$ is

$$\boldsymbol{\Sigma}^{\rm r}_{\rm L} = -\frac{\rm i}{2}\begin{pmatrix} \Gamma_{\rm L} & 0 & 0 & 0 \\ 0 & \Gamma_{\rm L} & 0 & 0 \\ 0 & 0 & 0 & 0 \\ 0 & 0 & 0 & 0 \end{pmatrix}, \quad (12)$$

where $\Gamma_{\rm L} = 2\pi|t_{\rm L}|^2\sum_k \delta(\omega - \varepsilon_{{\rm L}k})$. The term $\boldsymbol{\Sigma}^{\rm r}_{\rm R}$ is the self-energy from the coupling between the QD and the superconducting lead, and may be written as

$$\boldsymbol{\Sigma}^{\rm r}_{\rm R} = -\frac{\rm i}{2}\Gamma_{\rm R}\rho_{\rm s}(\omega)\begin{pmatrix} 1 & -\frac{\Delta}{\omega} & 0 & 0 \\ -\frac{\Delta}{\omega} & 1 & 0 & 0 \\ 0 & 0 & 0 & 0 \\ 0 & 0 & 0 & 0 \end{pmatrix}, \quad (13)$$

where $\Gamma_{\rm R} = 2\pi\rho_{\rm s0}|t_{\rm R}|^2$, with $\rho_{\rm s0}$ being the density of states when the superconductor is in the normal state, and $\rho_{\rm s}(\omega)$ is the modified BCS (Bardeen–Cooper–Schrieffer) density of states defined by

$$\rho_{\rm s}(\omega) = \frac{|\omega|\theta(|\omega| - \Delta)}{\sqrt{\omega^2 - \Delta^2}} + \frac{|\omega|\theta(\Delta - |\omega|)}{{\rm i}\sqrt{\Delta^2 - \omega^2}}. \quad (14)$$

Once the retarded Green's functions are known, the electric current can be calculated using Eqs. (8) and (9). In this work, we only consider the Andreev transport for energies within the superconducting gap. Thus, the current amplitude corresponding to the contribution of quasiparticle tunneling is zero. In particular, the zero-bias AR conductance at zero temperature can be calculated as[35]

$$G^{\rm A} = \frac{2e^2}{h}\sum_{i=1,3}^{j=2,4}\boldsymbol{G}^{\rm r}_{ij}(\Gamma_{\rm L}\boldsymbol{G}^{\rm a}\Gamma_{\rm L})_{ji}, \quad (15)$$

where $\boldsymbol{G}^{\rm a}$ is the advanced Green's function, $\boldsymbol{G}^{\rm a} = (\boldsymbol{G}^{\rm r})^\dagger$. It directly reflects the quantum interference in this system.

3. Results and discussion

In this section, we investigate the linear AR conductance at zero temperature in the N–QD–S system coupled with MBSs. In the numerical calculations discussed below, we consider a QD with only a single, spinless level of energy $\varepsilon_{\rm d}$. The Fermi energy and the energy level of the QD are restricted to lie within the energy gap of the superconducting lead.

We first illustrate the AR conductance as a function of the Fermi energy in the N–QD–S system. For comparison, the results for the N–QD–S systems with and without coupled MBSs are respectively shown in Figs. 2(a) and 2(b). We set $\Delta = 1$, $\varepsilon_{\rm d} = 0.2$, $\varepsilon_{\rm M} = 0.1$, and $\lambda = 0.1$. All parameters are expressed in units of the superconductor gap. For simplicity, we study only the symmetric case, and set $\Gamma_{\rm L} = \Gamma_{\rm R} = \Gamma$. In Figs. 2(a) and 2(b), the solid, dashed, and dotted lines denote $\Gamma = 0.05$, 0.15, and 0.25, respectively. It may be seen in Fig. 2(b) for the system without MBSs that the AR conductance curve exhibits two relatively weak peaks around the point $E_{\rm F} = \pm 0.2$. The magnitudes of the peaks are much smaller than e^2/h, though they increase as Γ increases. However, in the N–QD–S system with coupled MBSs, as shown in Fig. 2(a), the AR conductance curves exhibit double resonant peaks. The maximum conductance of the AR can reach as high

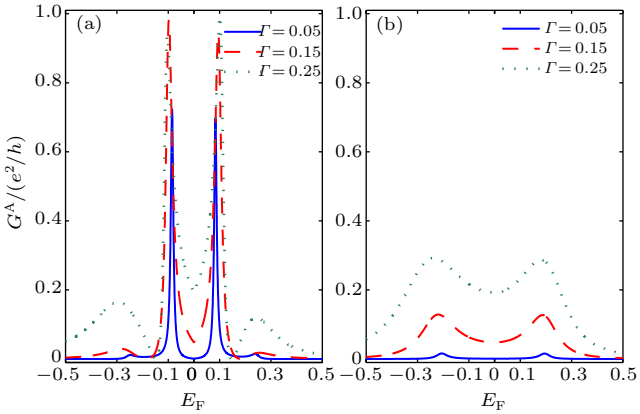


Fig. 2. (color online) AR conductance as a function of the Fermi energy in the N–QD–S systems (a) with and (b) without coupled MBSs. We set $\Delta = 1$, $\varepsilon_{\rm d} = 0.2$, $\varepsilon_{\rm M} = 0.1$, and $\lambda = 0.1$. All parameters are expressed in units of the superconductor gap.

as e^2/h, and is only slightly affected by the coupling strengths of the QD to the leads. In addition, we obtain the symmetric line shape because the AR involves both the particle and hole degrees of freedom. From Fig. 2, we can see that in the N–QD–S system, even though the AR conductance curves generally exhibit weak peaks when no MBSs are present, for appropriate tunnel coupling with the normal and superconducting leads, the AR can be enhanced when coupling to the MBSs is incorporated. Next, we analyze the AR in the N–QD–S system with coupled MBSs in more detail.

Figure 3 shows the AR conductance as a function of the Fermi energy in the N–QD–S system with coupled MBSs for different values of λ for the case of $\varepsilon_M = 0$ and $\varepsilon_d = 0$. From Fig. 3, we find several features of the AR conductance when only QD–MBS coupling is considered. First, in Fig. 3(a), for $\Gamma = 0.01$, we can clearly see four conductance peaks in each curve, located roughly symmetrically around the zero energy. In addition, the distance between the neighboring conductance peaks increases with increasing λ. When Γ increases from 0.01 to 0.1, as shown in Fig. 3(b), the conductance peaks are significantly suppressed, and one Fano line-shape appears in the AR conductance spectrum. These results can be easily understood. As shown in Fig. 1, the MBSs serve as a special electron reservoir with single energy mode. Electrons entering such a structure undergo phase randomization, thereby this tunneling channel is related to the dephasing mechanism. In practical terms, any decoherence is expected to suppressed the quantum features, therefore the stability of the Fano-type interference patterns can be regarded as a useful probe of an interplay between the coherence and incoherence tunneling channels. In this process, the AR conductance is always $e^2/2h$ at the point $E_F = 0$, showing the robust properties of the Majorana fermions.[14]

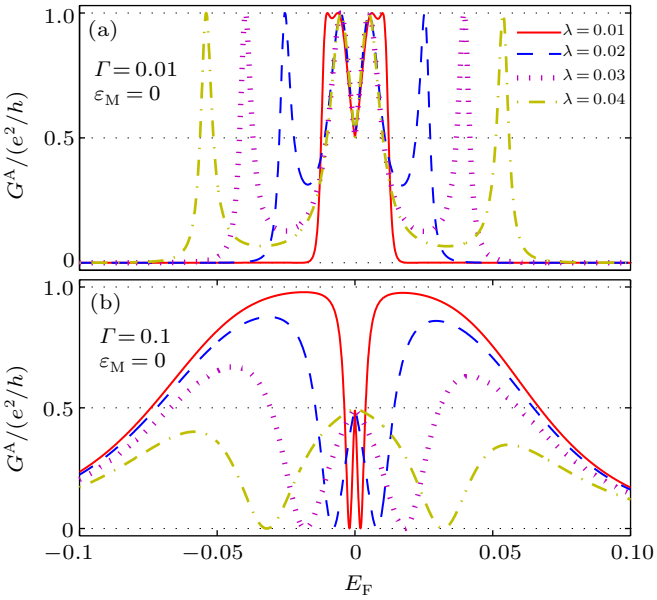


Fig. 3. (color online) AR conductance as a function of the Fermi energy in the N-QD-S system with coupled MBSs for different values of λ when $\varepsilon_d = 0$ and $\varepsilon_M = 0$: (a) $\Gamma = 0.01$, (b) $\Gamma = 0.1$.

Figure 4 shows the AR conductance as a function of the Fermi energy in the presence of not only the QD–MBS coupling but also the coupling between the two MBSs. The zero energy conductance deviates from $e^2/2h$ once $\varepsilon_M \neq 0$ as shown in Fig. 4. By a careful observation, one can also see that the coupling between the two MBSs widens the Fano resonance peak in Fig. 4(a) and the Fano antiresonance valley in Fig. 4(b). The N–QD–S structure with coupled MBSs provides two special transmission paths for the quantum interference. Therefore, the resonant channel for the Fano effect is simultaneously determined by both the weak QD–lead, QD–MBS coupling and the MBS–MBS coupling.

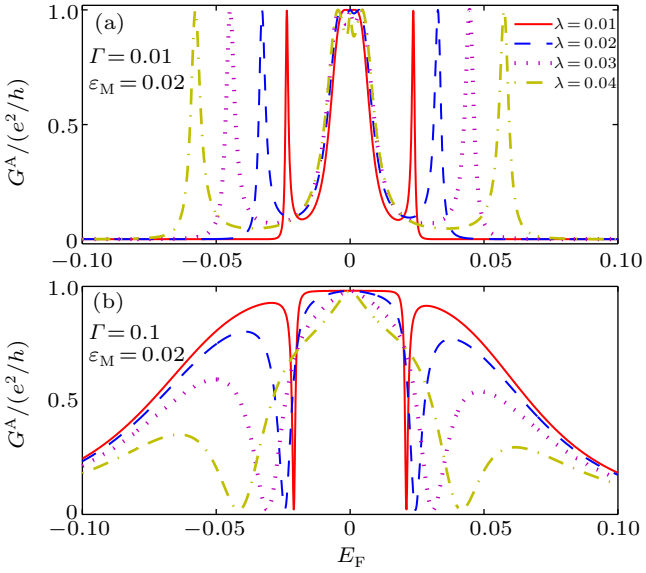


Fig. 4. (color online) AR conductance as a function of the Fermi energy in the N–QD–S system with coupled MBSs for different values of λ when $\varepsilon_d = 0$ and $\varepsilon_M = 0.02$: (a) $\Gamma = 0.01$, (b) $\Gamma = 0.1$.

Next, in Fig. 5, we illustrate the influence of changes in the MBS–MBS coupling on the AR conductance. In Fig. 5(a), when $\Gamma = 0.01$, one can see that the resonant peaks shift away from the zero Fermi energy point. In addition, one can see from Fig. 5(b) that when $\Gamma = 0.1$, the resonant line-shapes are greatly modified as ε_M increases. For example, in Fig. 5(b), the solid red line, $\varepsilon_M = 0.02$, is a small antiresonance with a peak at $E_F = 0$. With ε_M increasing to $\varepsilon_M = 0.06$ (see the blue dashed line in Fig. 5(b)), the original primary resonant peak becomes wider and the second peaks develop into a Fano line shape.

In order to obtain a better understanding of the above behaviors, in the following, we focus on under what conditions the Fano resonant AR might appear. In Fig. 6, we show the AR conductance at $E_F = \varepsilon_d = 0.1$ as a function of ε_M with different values of the QD–η_1 coupling λ for fixed $\Gamma = 0.2$. We can see that with these parameters, the AR conductance changes with ε_M. Obviously, there is a critical value ε_{Mc}. When $\varepsilon_M < \varepsilon_{Mc}$, the AR conductance decreases with increasing ε_M. When $\varepsilon_M > \varepsilon_{Mc}$, the AR conductance quickly increases from zero

to the maximum e^2/h, and then decreases to $e^2/2h$ slowly as ε_M increases further. The critical point is dependent on both λ and Γ. For fixed Γ, the critical value ε_{Mc} increases with decreasing λ. When $\varepsilon_M = 0.1$, which just equals to the energy level of the QD, the resonant AR occurs quickly and gives the maximum AR conductance; when ε_M deviates from this point, the AR conductance quickly decreases to $e^2/2h$.

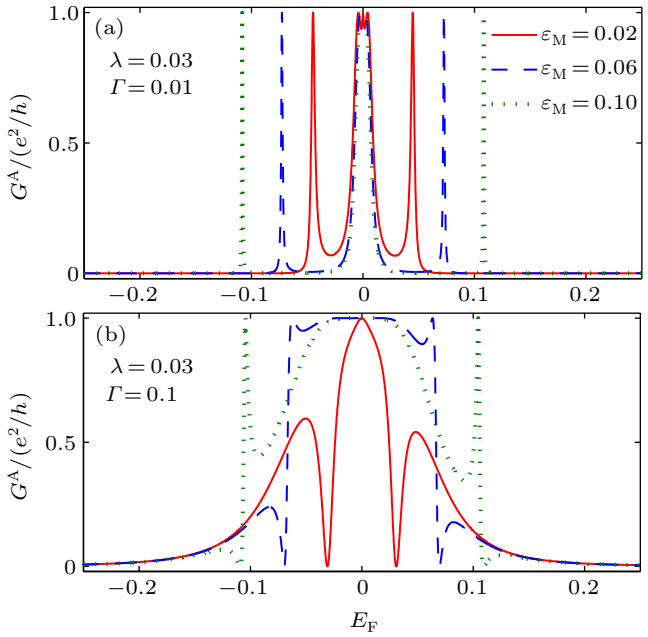


Fig. 5. (color online) AR conductance as a function of the Fermi energy in the N–QD–S system with coupled MBSs for different values of ε_M when $\varepsilon_d = 0$ and $\lambda = 0.03$: (a) $\Gamma = 0.01$, (b) $\Gamma = 0.1$.

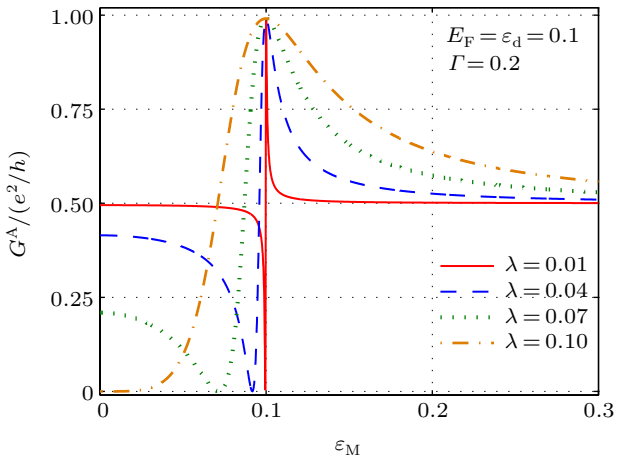


Fig. 6. (color online) AR conductance as a function of ε_M in the N–QD–S system with coupled MBSs for different values of λ when $E_F = \varepsilon_d = 0.1$ and $\Gamma = 0.2$.

We also calculate the AR conductance as a function of λ for different values of ε_M for the case of $\Gamma = 0.2$ and $E_F = \varepsilon_d = 0.1$. The results are shown in Fig. 7. When $\varepsilon_M = \varepsilon_d$ (see the black dot-dashed line in Fig. 7), an intense resonance occurs, and the AR conductance increases quickly from the initial value $e^2/2h$ to the maximum e^2/h. When $\varepsilon_M > \varepsilon_d$, G^A increases gradually from $e^2/2h$ to e^2/h with increasing λ. However, for $\varepsilon_M < \varepsilon_d$, there is a critical value of λ, λ_c, corresponding to $G^A = 0$. When $\lambda < \lambda_c$, G^A decreases from $e^2/2h$ to zero with increasing λ. Once $\lambda > \lambda_c$, G^A increases gradually from zero to its maximum and remains at the maximum value with a further increase in λ.

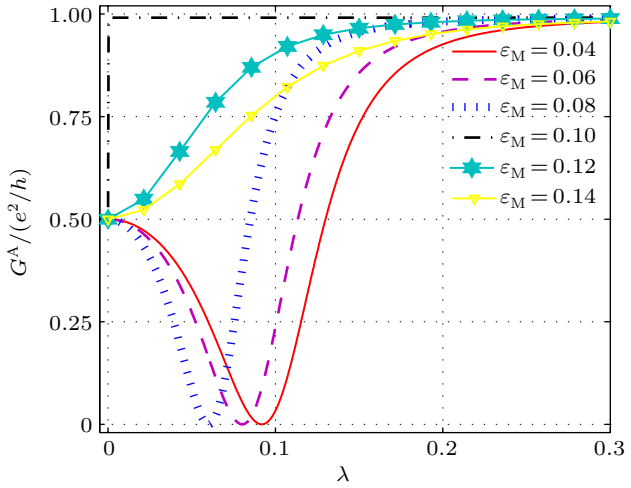


Fig. 7. (color online) AR conductance as a function of λ in the N–QD–S system with coupled MBSs for values of ε_M when $E_F = \varepsilon_d = 0.1$ and $\Gamma = 0.2$.

4. Summary

We have studied the AR in an N–QD–S system coupled with MBSs. We found that for appropriate tunnel coupling with the normal and superconducting leads, the AR is enhanced by the MBSs. For a given Fermi energy, one can tune the gate voltage to obtain a primary resonant state. One can then change the coupling strength between the QD and the MBS η_1 or between the two MBSs to obtain a Fano resonance. The AR conductance is always $e^2/2h$ at the zero energy point when only QD–MBSs coupling is considered, showing the robust properties of the Majorana fermions. In addition, with strong QD–MBS coupling, the resonant AR can occur even in the absence of coupling between the two MBSs. When the MBS–MBS coupling roughly equals to the QD energy level, the resonant AR can also occur even with very weak QD–MBS coupling. We also found that an AR antiresonance appears when the QD energy level approximately equals to the sum of the QD–MBS coupling and the MBS–MBS coupling. Based on all the numerical results, we propose that such a system may be a candidate for detecting the MBSs. Furthermore, these results will be helpful for understanding the quantum interference in MBS-assisted AR and may find significant applications, especially in quantum computation.

References

[1] Majorana E 1937 *Nuovo Cimento* **14** 171
[2] Alicea J, Oreg Y, Refael G, von Oppen F and Fisher M P A 2011 *Nat. Phys.* **7** 412
[3] Das A, Ronen Y, Most Y, Oreg Y, Heiblum M and Shtrikman H 2012 *Nat. Phys.* **8** 887

[4] Leijnse M and Flensberg K 2011 *Phys. Rev. Lett.* **107** 210502
[5] Zhang D P amd Tian G S 2015 *Chin. Phys. B* **24** 080401
[6] Fu L and Kane C L 2008 *Phys. Rev. Lett.* **100** 096407
[7] Sau J D, Lutchyn R M, Tewari S and Das Sarma S 2010 *Phys. Rev. Lett.* **104** 040502
[8] Mourik V, Zuo K, Frolov S M, Plissard S R, Bakkers E P A M and Kouwenhoven L P 2012 *Science* **336** 1003
[9] Chen W, Xue Z Y, Wang Z D and Shen R 2014 *Chin. Phys. B* **23** 030309
[10] Oreg Y, Refael G and von Oppen F 2010 *Phys. Rev. Lett.* **105** 177002
[11] Lutchyn R M, Sau J D and Das Sarma S 2010 *Phys. Rev. Lett.* **105** 077001
[12] Deng M T, Yu C L, Huang G Y, Larsson M, Caroff P and Xu H Q 2012 *Nano Lett.* **12** 6414
[13] Flensberg K 2011 *Phys. Rev. Lett.* **106** 090503
[14] Liu D E and Baranger H U 2011 *Phys. Rev. B* **84** 201308
[15] Li Y X and Bai Z M 2013 *J. Appl. Phys.* **114** 033703
[16] Wang N, Lv S H and Li Y X 2014 *J. Appl. Phys.* **115** 083706
[17] Deng M X, Zheng S H, Yang M, Hu L B and Wang R Q 2015 *Chin. Phys. B* **24** 037302
[18] Lü H F, Lu H Z and Shen S Q 2014 *Phys. Rev. B* **90** 195404
[19] Gong W J, Zhang S F, Li Z C, Yi G Y and Zheng Y S 2014 *Phys. Rev. B* **89** 245413
[20] Lü H F, Guo Z, Ke S S, Guo Y and Zhang H W 2015 *J. Appl. Phys.* **117** 164312
[21] Leijinse M and Flensberg K 2011 *Phys. Rev. B* **84** 140501
[22] Shang E M, Pan Y M, Shao L B and Wang B G 2014 *Chin. Phys. B* **23** 057201
[23] Chen Wei, Xue Z Y, Wang Z D and Shen R 2014 *Chin. Phys. B* **23** 030309
[24] Zhou Y and Guo J H 2015 *Acta Phys. Sin.* **64** 167302 (in Chinese)
[25] Nilsson J, Akhmerov A R and Beenakker C W J 2008 *Phys. Rev. Lett.* **101** 120403
[26] Zocher B and Rosenow B 2013 *Phys. Rev. Lett.* **111** 036802
[27] Fazio R and Raimondi R 1998 *Phys. Rev. Lett.* **80** 2913
[28] Sun Q F, Wang J and Lin T H 1999 *Phys. Rev. B* **59** 3831
[29] Sun Q F, Wang J and Lin T H 2001 *Phys. Rev. Lett.* **87** 176601
[30] Barański J and Domański T 2015 *Chin. Phys. B* **24** 017304
[31] Li Y X 2008 *Chin. Phys. Lett.* **25** 3739
[32] Fano U 1961 *Phys. Rev.* **124** 1866
[33] Reimann S M and Manninen M 2002 *Rev. Mod. Phys.* **74** 1283
[34] Cuevas J C, Martín-Rodero A and Levy Yeyati A 1996 *Phys. Rev. B* **54** 7366
[35] Haug H and Jauho A P 1998 *Quantum Kinetics in Transport and Optics of Semiconductors* (Berlin: Springer-Verlag)